Journal of Alloys and Compounds 499 (2010) 63–67

Contents lists available at ScienceDirect

Journal of Alloys and Compounds

journal homepage: www.elsevier.com/locate/jallcom

Effect of electron irradiation on properties of chemically deposited TiO_2 nanorods

D.S. Dhawale [a], D.P. Dubal [a], R.R. Salunkhe [a], T.P. Gujar [a], M.C. Rath [b], C.D. Lokhande [a,*]

[a] Thin Film Physics Laboratory, Department of Physics, Shivaji University, Kolhapur 416004, India
[b] Radiation & Photochemistry Division, Bhabha Atomic Research Centre, Trombay, Mumbai 400085, India

ARTICLE INFO

Article history:
Received 22 December 2009
Received in revised form 22 January 2010
Accepted 22 January 2010
Available online 2 February 2010

Keywords:
CBD
TiO_2
Nanorods
Thin films
Electron irradiation

ABSTRACT

TiO_2 nanorods were grown by using soft chemical route at room temperature on glass substrate and subjected to electron beam irradiation after annealing for 2 h in air at 723 K. The effect of annealing and high energy (7 MeV) electron beam irradiation on the structural, morphological, wettability, optical and electrical properties of the films has been investigated. The electron bombardment leads amorphous to crystalline structure, increase in length and diameter of nanorods, increase in contact angle from 2° to 9°, red shift of 0.24 eV in the band gap and decrease in room temperature electrical resistivity from 10^6 to 10^3 of TiO_2 nanorods. The changes in the material property are ascribed to the effect of electron beam irradiation.

1. Introduction

Titanium dioxide (TiO_2) is one of the most attractive, technological important and extensively studied transition-metal oxides for diverse applications. The increased interest in both the application and the fundamental research of this material in the last decade stems from its remarkable optical and electronic properties. It has typical properties such as transparency in the visible range, high-electrochemical stability, direct band gap (3.2 eV), exhibiting n-type conductivity, absence of toxicity, abundance in nature, easy handling thus making TiO_2 for large area of applications. Nanocrystalline TiO_2 has been extensively investigated, as it plays a prominent role in fundamental studies and has both potential and practical applications in solar energy conversion [1], photocatalysis [2], photochromic devices [3], and gas sensors [4,5]. Although, the commercial methods of TiO_2 thin film fabrication used today are the gas phase techniques such as sputtering [6], and MOCVD [7], many workers have employed in low cost soft solution chemical methods for the preparation of TiO_2 thin films [8–11]. Physical methods are suitable for the growth of uniform and high quality films, but they are expensive. On the other hand, chemical methods are economic and porous structures with high surface area can be grown with simplicity. For the deposition of the TiO_2 thin films, among the chemical deposition methods, most of the researchers have fascination towards the chemical bath deposition (CBD) due to its simplicity and low cost, besides the capability to achieve large area coating. It is understood from the literature that much attention is not focused on the deposition of TiO_2 nanorods prepared by CBD method.

Currently, TiO_2 thin films are expected to play a significant role in nano- and microtechnologies. Therefore, more and more efforts are performed in order to develop methods for nano- or microstructuring of TiO_2 thin films. The commonly employed post-treatment methods are laser irradiation [12,13], ion bombardment [14], and electron beam irradiation [15]. Although few works on the electron irradiation effect in a TiO_2 films are available, most of them deal with the improvement of the TiO_2 photoactivity as a function of the absorbed radiation dose (MGy) [16]. However, effect of electron bombardment on the material properties of TiO_2 thin films has not been addressed in detail.

In this study, an attempt has been addressed to enlighten the electron irradiation effects on the structural, morphological wettability, optical and electrical properties of electron bombarded TiO_2 nanorods grown by chemical bath deposition. We also showed that the enhanced crystallinality, increase in diameter and length of nanorods, decrease in optical band gap and electrical resistivity of TiO_2 nanorods are largely due to the changes in the material property upon electron irradiation.

2. Experimental details

2.1. Sample preparation

Unless otherwise noted, AR chemicals were obtained from commercial suppliers and used without further purification. Nanorods of TiO_2 were grown onto the glass substrate by soft chemical bath deposition (CBD) in aqueous acidic medium at the room temperature (300 K). Specifically, 2.5 ml titanium (III) chloride solution

* Corresponding author. Tel.: +91 231 2609229; fax: +91 0231 2692333.
E-mail address: l.chandrakant@yahoo.com (C.D. Lokhande).

0925-8388/$ – see front matter © 2010 Elsevier B.V. All rights reserved.
doi:10.1016/j.jallcom.2010.01.126

(30 wt% in HCl) was added to 50 ml double distilled water as a titanium source. For the complex formation, 0.1 M urea (NH_2CONH_2) was added with constant stirring for 30 min, and pH adjusted to ~1. After stirring homogeneous violet solution was kept under unstirred condition and precleaned with detergent solution and ultrasonically treated glass substrates were immersed in the bath at room temperature. This clear solution was kept under unstirred condition and glass substrate was dipped in it for 72 h. Whitish films due to the $Ti(OH)_4$ were formed on glass substrate. The $Ti(OH)_4$ films were heat treated in oxygen air-tight container at 723 K for 2 h for the removal of hydroxyl phase which generally facilitates decrease in dislocations, stresses, inhomogeneities. Finally, $Ti(OH)_4$ films were changed to TiO_2 after annealing. The synthesized films were specularly reflecting, uniform and well adherent to the substrates. Annealed films were subjected to electron beam irradiation.

2.2. Irradiation experiment

The TiO_2 films were irradiated with electron beam from a 7 MeV linear electron accelerator (LINAC) set-up at the Bhabha Atomic Research Centre (BARC), Mumbai, India; the details are described elsewhere [17]. The TiO_2 film samples were kept in front of the exit of the LINAC at a distance of 12 cm where the liquid samples (cell dimensions: 10 mm × 10 mm × 50 mm) are kept for the pulse radiolysis study. The dose absorbed by aqueous solutions per pulse was determined using a chemical dosimeter, an aerated aqueous solution containing 1×10^{-2} mol dm^{-3} potassium thiocyanate (KSCN) [18]. This dose value was used to calculate the total dose delivered in a sample under a repetitive irradiation condition. Electron pulses of 2 μs time duration with a peak current, 70 mA were used for the irradiation of the sample. The electron flux was about 3×10^{12} electrons/2 μs/cm^2. The sample was irradiated by the electron pulses at a repetition rate of 12 pulses/s for about 6.5 s, accounting for a cumulative dose of about 10 kGy.

2.3. Characterization techniques

The thickness of the film was measured using fully computerized AMBIOS Make XP^{-1} surface profiler with 1 Å vertical resolution. The maximum thickness obtained for TiO_2 thin film was 0.2 μm. The as-deposited, annealed and irradiated TiO_2 films were used for further characterizations. The crystal structural characterization of films was studied by using Philips PW-1710 X-ray diffractometer with Cu-Kα radiation (λ = 1.5406 Å). Surface morphology was investigated using high-resolution scanning electron microscopy (FE-SEM, Model: JSM-6160) at an acceleration voltage higher than 5 kV. Samples were coated with a 10 nm Au layer prior to analysis to prevent charging. The static contact angle against water was measured using a contact angle meter (Rame-Hart, USA) with CCD camera that is equipped with this contact angle meter (CA-X) used to observe the shape of water drop on the surface of the TiO_2 film. Droplet was placed at five different positions for one sample and the averaged value was adopted as the contact angle. For the optical studies, UV–vis absorption spectra were measured on a double beam spectrophotometer (CHEMITO 2600) with glass substrate as a reference in the wavelength range of 350–850 nm. To study the electrical characterization of the films, dark electrical resistivity measurements were carried out using dc two-probe method in the range of 300–600 K.

3. Results and discussion

3.1. Film formation mechanism

In chemical bath deposition method, film formation observed when the solution is saturated, the ionic product of anion and cation is equal to solubility product of metal oxide and when it exceeds, precipitation occurs and ions combine on the substrate and in the solution to form nuclei. Depending upon the optimized preparative conditions such as bath temperature, pH of resultant solution, deposition time, solution concentration, the film growth can take place by ion-by-ion condensation of materials or by the adsorption of colloidal particles from the solution on the substrate. The formation of solid phase from a solution involves two steps as nucleation and particle growth.

TiO_2 films have been deposited on glass substrate by the chemical reaction using urea can be enlightened as follows.

Initially TiC_{l3} dissociates into as per reaction (1):

$$TiCl_3 \rightarrow Ti^{3+} + 3Cl^- \quad (1)$$

The decomposition of urea can be expressed below:

$$NH_2CONH_2 + 3H_2O \rightarrow 2NH_4OH + CO_2 \quad (2)$$

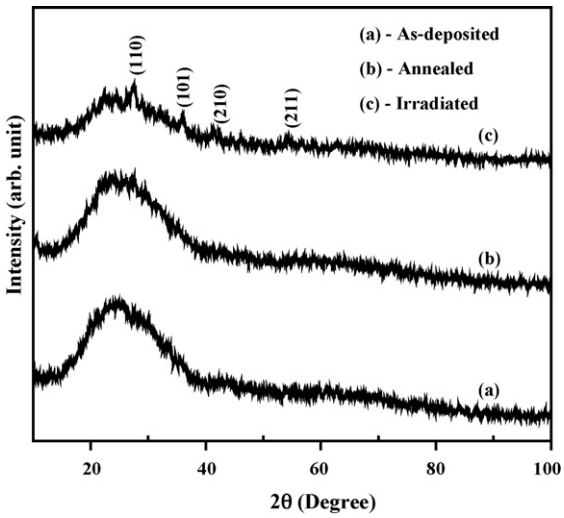

Fig. 1. The X-ray diffractograms of (a) as-deposited (b) annealed, and (c) electron beam irradiated TiO_2 films.

As indicated in Eq. (2), 1 mole of the urea produces 2 moles of the ammonia in the decomposition process. Such produced ammonia can react with a $TiCl_3$ in the presence of water. In water, the produced ammonia breaks down into an ammonium ion and a hydroxide ion, as per the reaction

$$NH_4OH \rightarrow NH_4^+ + OH^- \quad (3)$$

The resulting NH_4^+ ion can react with a Cl_3 and forms salt. While OH^- ion can react with a Ti^{3+} resulting in a titanium hydroxide, which is useful for producing the titanium oxide as per the reaction,

$$3Cl^- + 3NH_4^+ \rightarrow 3NH_4Cl \quad (4)$$

$$4Ti^{3+} + 16(OH)^- \rightarrow 4Ti(OH)_4 \quad (5)$$

After annealing at temperature 723 K in air, as-deposited $Ti(OH)_4$ films converted into TiO_2 by following the chemical reaction,

$$Ti(OH)_4 \xrightarrow{\Delta 723\ K} TiO_2 + 2H_2O \quad (6)$$

3.2. Structural studies

Fig. 1(a–c) shows the X-ray diffraction patterns of as-deposited, annealed and electron irradiated TiO_2 thin films, respectively. The XRD patterns of the both the as-deposited and annealed TiO_2 film displays only broad hump peak. The characteristic broadening of the observed peaks implies that the films are nanocrystalline or amorphous nature, similar to results reported by Kale et al. [19] by SILAR approach. Interestingly, upon electron irradiation of dose 10 kGy, sharp and narrow peaks are observed which results into the increase in crystallinity with peaks corresponding to (1 1 0), (1 0 1), (2 1 0) and (2 1 1) plane of reflections are in good agreement with the Joint Committee on Powder Diffraction Standard (JCPDS) (No. 84-1284), confirming the formation of nanocrystalline TiO_2 of rutile phase. The presence of several peaks indicates a random orientation of crystallites in the film. Though irradiation is known to induce disorder in the structure, we observe improvement in crystalline size. The improvement in the crystalline structure during electron irradiation can be explained by diffusion towards the surface of the non-stoichiometric atoms (in semiconductor compounds), which exist in a free state among the crystallites at dislocation, microfissures, etc. The diffusion of these atoms and their elimination from the film are considerably favoured during irradiation. While migrating through the sample under the effect of radiation,

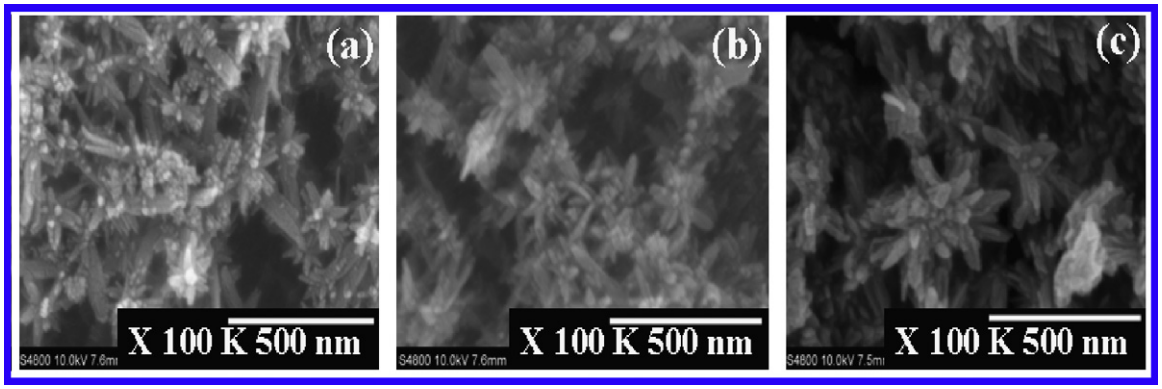

Fig. 2. The FESEMs of (a) as-deposited (b) annealed, and (c) electron beam irradiated TiO_2 films at magnification 100K×.

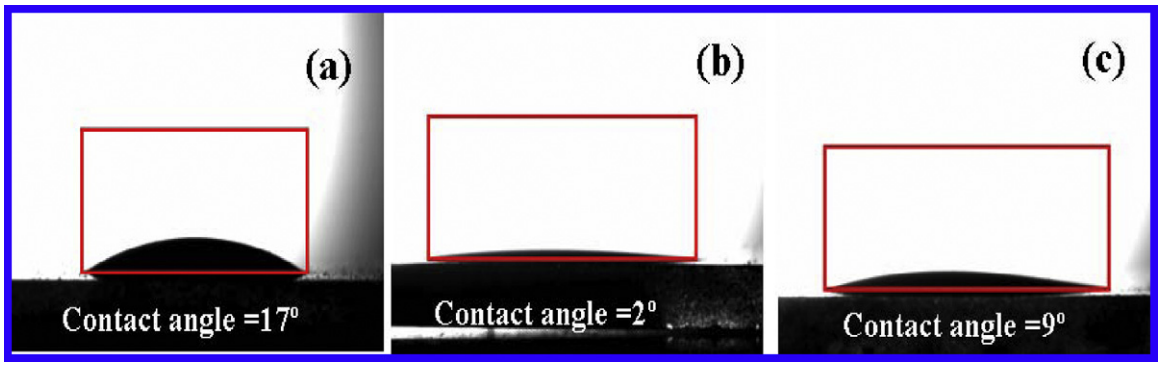

Fig. 3. The photoimages of contact angle measurement of (a) as-deposited (b) annealed, and (c) electron beam irradiated TiO_2 films.

the non-stoichiometric atoms may fill vacancies in the crystalline lattice, thus leading to an improvement in its structure.

3.3. Surface morphological studies

The two-dimensional surface morphological study of the TiO_2 films has been carried out using FESEM images. Fig. 2(a–c) shows the FESEM images of as-deposited, annealed and electron irradiated TiO_2 thin films, respectively at magnification 100K×. From Fig. 2(a and b) it is revealed that both the as-deposited and annealed films are amorphous in nature with little grain size improvement after annealing is observed. However, for electron irradiated TiO_2 film considerable growth of nanorods is easily seen (Fig. 2(c)). The mean diameter for TiO_2 nanorods is of the order ~0.2 μm while length typically ranges from 0.5 to 1 μm for irradiated films.

3.4. Surface wettability

Wettability involves the interaction between a liquid and a solid in contact. Wetting is an important property of a surface and is controlled by both the chemical nature and the geometrical structure. Fig. 3(a–c) shows photoimages of contact angle measurement with the nanocrystalline TiO_2 surfaces and a water droplet for as-deposited, annealed and electron irradiated, respectively. The as-deposited TiO_2 thin films shows a contact angle of about 17° which decreases after annealing to 2° indicating that TiO_2 is a superhydrophilic material. Interestingly, upon electron irradiation further water contact angle increases to 9°. Upon electron irradiation, surface roughness increases which exhibits more water contact angle. Both super-hydrophilic and super-hydrophobic surfaces are important for practical applications [20]. In the present case, the water lies flat instead of forming droplet which is attributed due to nanocrystalline nature that is expected to possess very high surface energy, which increases with the reduction in particle size [21]. Upon electron irradiation, surface roughness increases which exhibits more contact angle as compared with pristine TiO_2 film surface.

3.5. Optical absorption studies

The optical absorption spectra of TiO_2 films deposited onto a glass substrate were studied at room temperature in the range of wavelengths 350–850 nm. Fig. 4(a–c) shows the variation of optical absorbance (αt) with wavelength (λ) of as-deposited, annealed and electron irradiated TiO_2 films, respectively. It is clearly seen from the optical spectra that the increase in optical absorption along with edge shifts towards a longer wavelength for irradiated films indicating that electron irradiation technique can be used to

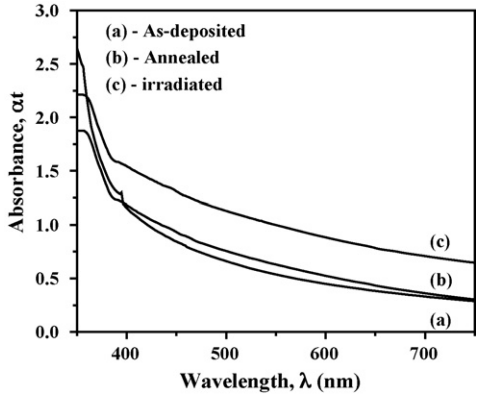

Fig. 4. The variation of optical absorbance (αt) vs. wavelength (λ) of (a) as-deposited (b) annealed, and (c) electron beam irradiated TiO_2 films.

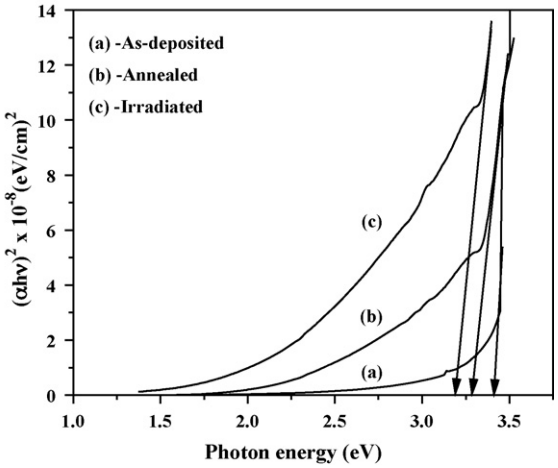

Fig. 5. The variation of $(\alpha h\upsilon)^2$ vs. $h\upsilon$ to determine the direct band gap of (a) as-deposited (b) annealed, and (c) electron beam irradiated TiO_2 films.

modify film properties in a controlled manner. This shift indicates that decrease in the optical band gap 'E_g'. The fundamental absorption, which corresponds to electron excitation from the valence band to conduction band, can be used to determine the nature and value of the optical band gap. The relation between the absorption coefficient (α) and the incident photon energy ($h\upsilon$) can be written as,

$$\alpha h\upsilon = \alpha_0(h\upsilon - E_g)^n \quad (7)$$

where α is the absorption coefficient, α_o is a constant, E_g is the band gap, and n is equal to 1/2 for a direct and 2 for indirect transition. The band gap can be estimated from a plot of $(\alpha h\upsilon)^2$ vs. photon energy ($h\upsilon$). The intercept of the tangent to the plot will give a good approximation of the band gap energy for this direct band gap material shown in Fig. 5. It is found to be 3.42 eV for as-deposited (Fig. 5(a)) and for annealed it is about 3.28 eV (Fig. 5(b)) which becomes 3.18 eV after electron irradiation (Fig. 5(c)) which is very close to the value reported earlier [15]. Clearly, there is a red shift (0.24 eV) in the band gap. Such a red shift in the band gap could be accounted either by the improvement in the crystallinity of the films by the possible increase in the oxygen vacancies or titanium vacancies due to electron bombardment.

3.6. Resistivity studies

Fig. 6(a–c) shows the plot of logarithmic resistivity vs. the inverse of temperature for as-deposited, annealed and electron beam irradiated TiO_2 films. From the plot it is clear that the resistivity decreases with increase in temperature indicating semiconducting behavior of these films. From Fig. 6(a and b) it is concluded that as-deposited and annealed TiO_2 films do not show two regions which might be due to the amorphous structure which is a most commonly observed phenomenon with high room temperature resistivity (1.58×10^6 for as-deposited and $9.33 \times 10^4\ \Omega$ cm for annealed TiO_2 films). Electron beam irradiation causes a sharp decrease in resistivity ($3.16 \times 10^3\ \Omega$ cm) which may be due to the partial dissociation of the oxide to provide excess titanium [22]. From Fig. 6(c), it is clearly seen that the resistivity of the film has two distinct conduction mechanisms. The transition from a straight line region with a low gradient to one with a higher gradient as temperature is increased suggests that more than one conduction mechanism are involved. The electrical resistivity decreased after irradiation is due to the improvement in crystallite size, decreases in (1) density of grain boundary intercrystallite, (2) grain boundary discontinuities, (3) defects such as pinholes, voids, etc., and (4) improvement of nanoparticle size and/or recrystallization of TiO_2 films. The well-known exponential law can describe the temperature dependence of the electrical resistivity.

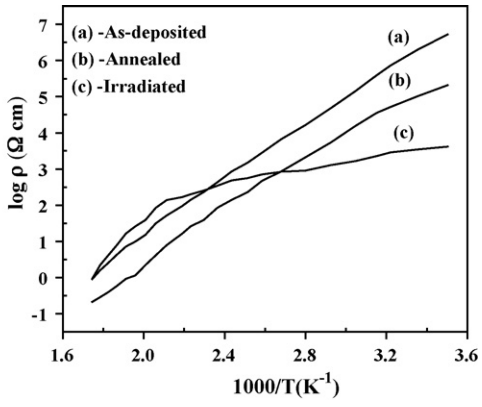

Fig. 6. Plot of log ρ vs. 1000/T of (a) as-deposited (b) annealed, and (c) electron beam irradiated TiO_2 films (the plot shows two regions).

$$\rho = \rho_0 \exp\left(\frac{E_a}{KT}\right) \quad (8)$$

where ρ is the resistivity at temperature T, ρ_0 is a parameter depending on the sample characteristics (structure, thickness, etc.) constant, K the Boltzmann's constant, E_a denotes the thermal activation energy of electrical conduction and T is the absolute temperature. The activation energy represents the location of trap levels below the conduction band. For as-deposited and annealed TiO_2 film, the activation energies are found to be 0.075 eV and 0.07 eV, respectively. In the case of irradiated TiO_2 films, $E_a = 0.035$ eV for low temperature (1st region) and $E_a = 0.012$ eV for high temperature (2nd region). The decrease in the dc activation energy may be attributed to the enhanced tailing of the valence band due to change in the electronic structure as well as defects creation, caused by the irradiation.

4. Conclusions

To summarize, we have reported on the effect of electron beam irradiation on the properties of TiO_2 thin films. The structural, morphological, wettability, optical and electrical properties of the TiO_2 film are modulated by electron bombardment. (i) The as-prepared amorphous TiO_2 film is crystallized by electron beam irradiation, (ii) increase in diameter and length of nanorods (iii) increase in contact angle from 2° to 9°, (iv) the band gap is red shifted by 0.24 eV and (v) decrease in room temperature resistivity by three orders of magnitude. All these changes in the material properties are attributed to the surface heating of the film induced by electron bombardment.

Acknowledgements

Authors are grateful to the Department of Science and Technology, New Delhi for financial support through the scheme no. SR/S2/CMP-82/2006. Authors acknowledge to Dr. S.K. Sarkar, Head, RPCD, BARC and the LINAC group for their support and help for this irradiation studies.

References

[1] B.O. Regan, M. Gratzel, Nature 353 (1991) 737.
[2] M.R. Hoffmann, S.T. Martin, W. Choi, D.W. Bahnemann, Chem. Rev. 95 (1995) 69.
[3] K. Naoi, Y. Ohko, T. Tatsuma, J. Am. Chem. Soc. 125 (2003) 3664.

[4] Y. Zhu, J. Shi, Z. Zhang, C. Zhang, X. Zhang, Anal. Chem. 74 (2002) 120.
[5] N. Wu, S. Wang, I.A. Rusakova, Science 285 (1999) 1375.
[6] H. Irie, S. Washizuka, K. Hashimota, Thin Solid Films 510 (2006) 21.
[7] A. Monoy, A. Brevet, L. Imhoff, B. Domenichini, E. Lesniewska, P.M. Peterle, M.C. Macro de Lucas, S. Bourgeois, Thin Solid Films 515 (2006) 687.
[8] R.S. Mane, Y.H. Hwang, C.D. Lokhande, S.D. Sartale, S.H. Han, Appl. Surf. Sci. 246 (2005) 271.
[9] C.D. Lokhande, E.H. Lee, K.D. Jung, O.S. Joo, J. Mater. Sci. 39 (2004) 2915.
[10] B.R. Sankapal, M.Ch. Lux-Steiner, A. Ennaoui, Appl. Surf. Sci. 239 (2005) 165.
[11] H.M. Pathan, S.K. Min, J.D. Desai, K.D. Jung, O.S. Joo, Mater. Chem. Phys. 97 (2005) 5.
[12] O.V. Overschelde, R. Snyders, M. Wautelet, Appl. Surf. Sci. 254 (2007) 971.
[13] W.M. Steen, Laser Material Processing, Springer, Berlin, 2005.
[14] M. Thakurdesai, A. Mahadkar, P.K. Kulriya, D. Kanjilal, V. Bhattacharyya, Nucl. Instrum. Methods Phys. Res. B 266 (2008) 1343.
[15] X.G. Houa, A.D. Liua, Radiat. Phys. Chem. 77 (2008) 345.
[16] J. Jun, M. Dhayal, J.H. Shin, J.C. Kim, N. Getoff, Radiat. Phys. Chem. 75 (2006) 583.
[17] S.N. Guha, P.N. Moorthy, K. Kishore, D.B. Naik, K.N. Rao, Proc. Indian Acad. Sci. (Chem. Sci.) 99 (1987) 261.
[18] M.C. Rath, Y. Sunitha, H.N. Ghosh, S.K. Sarkar, T. Mukherjee, Radiat. Phys. Chem. 78 (2009) 77.
[19] S.S. Kale, R.S. Mane, H. Chung, M.Y. Yoon, C.D. Lokhande, S.H. Han, Appl. Surf. Sci. 253 (2006) 421.
[20] R.D. Sun, A. Nakajima, A. Fujushima, T. Watanabe, K. Hashimoto, J. Phys. Chem. B 105 (2001) 1984.
[21] P.G. de Gennes, Rev. Modern Phys. (1985) 830.
[22] L. Holland, G. Siddall, Vacuum 3 (1953) 373.